

THE ORBITAL AND PHYSICAL PARAMETERS OF THE ECLIPSING BINARY OW GEMINORUM

*By C. Gałan¹, M. Mikołajewski¹, T. Tomov¹, D. Kolev², D. Graczyk¹,
A. Majcher^{1,3}, J. L. Janowski¹ and M. Cikala^{1,4}*

¹*Uniwersytet Mikołaja Kopernika, Centrum Astronomii, Toruń, Polska*

²*National Astronomical Observatory Rozhen, Institute of Astronomy, Smolyan, Bulgaria*

³*Instytut Problemów Jądrowych im. Andrzeja Soltana Otwock – Świerk, Warszawa, Polska*

⁴*Obserwatorium Astronomiczne im. T. Banachiewicza, Węglówka, Polska*

We present our multicolour photometric data of the primary and secondary eclipses of OW Gem that took place in 1995, 2002, and 2006, as well as new radial-velocity data collected since 1993 by R. F. Griffin and A. Duquennoy. The Wilson–Devinney code was used for the simultaneous solution of both photometric and spectroscopic data. A complete set of orbital and physical parameters of the components was obtained. The pair of values, eccentricity $e = 0.5286$ and argument of periastron $\omega = 140^\circ.73$, give better compatibility of the moment of the secondary minimum with the observations compared to previous estimates.

Introduction.

OW Gem is an unusual, long-period eclipsing binary, composed of two evolved supergiant stars. Variability of the star has been noticed by Kaiser¹ during photographic searches of nova stars in March 1988. Photoelectric observation soon showed a shallow secondary minimum² at phase 0.23 in the V band, indicating that the orbit has high eccentricity. It turned out that eclipses were visible on Harvard photographic plates³ already from 1902. The orbital period (1258.59 days - about 3.45 years) was derived from 11 eclipse events, which took place before 1992⁴. Radial velocity data of very good quality were obtained by Griffin & Duquennoy⁵ (in tables: G&D), and used by them for the first reliable analysis of the system. The presence of eclipses distinguish OW Gem from several known similar systems⁶, hence we know the exact masses of the components in this case ($5.5M_{\odot}$ and $3.8M_{\odot}$). The object has turned out to be unusually interesting. Both its components have quite large, but considerably different masses and they are now simultaneously in the short phase of supergiant evolution. Therefore, the evolutionary status of the system seems to be in contradiction to the current stellar evolutionary models.

Many attempts of modelling the system parameters appeared in recent years as a result of several authors carrying out good quality multicolour photometric measurements

of the eclipses. Derekas *et al.*⁷ have presented a simple model based on observations of the main minimum at the turn of the years 2001 and 2002, in which they estimate the temperature and the luminosity of the components. Another group (Terrell *et al.*⁸) has used Wilson – Devinney code (hereafter: WD) for modelling and operating on Kaiser *et al.*⁹ photoelectric observational data together with the only available at that time radial velocity measurements⁵, and they have obtained a complete set of parameters. In the same year, we presented a simple model¹⁰ within the confines of which we have obtained the inclination of the orbit and the most probable temperature $T_2 = 4950K$ of the secondary (cool) component for an assumed value of the primary temperature $T_1 = 7100K$. In that model, the limb darkening was neglected and stellar fluxes were approximated as blackbodies. This work presents new multicolour photometry covering one (1995) primary eclipse and three (1995, 2002, 2006) secondary eclipses. We have independently obtained a complete set of parameters using our own and part of Derekas *et al.*⁷ photometric data. The new - partly not published earlier - radial velocity data (Appendix – Table 12) were used, due to kindness of Roger Griffin which has collected them together with A. Duquennoy during the last fourteen years. Suggested by Dr R.F. Griffin weight were applied. Additionally three our own radial velocity measurements (Appendix – Table 13) were included for analysis.

Observational photometric data

An international observational campaign was organized by Terrell *et al.* during 1995 primary and secondary eclipses¹¹. Responding to this, we obtained multicolour photometry for both events with a 60 cm Cassegrain reflector at Piwnice Observatory near Toruń (Poland). We used a single-channel diaphragm photometer with non – cooled EMI 9558B photomultiplier. Our response curves for U , B and V bands were very close to the standard Johnson's system, whereas our broad R , I bands had significantly shorter mean wavelengths than Johnson RI and Cousins $(RI)_C$ (Table 1). The accuracy of our measurements was ± 0.03 , ± 0.02 , ± 0.017 , ± 0.02 and ± 0.019 in $UBVRI$ respectively. Unfortunately, in the analysis based on the 1995 campaign⁹ our photometric data were not included. Our observations of the 1995 secondary eclipse have poor time covering as a result of bad weather. To fill the gaps in the light curves, new data were obtained nearby and during the 2002 secondary eclipse. A single-channel diaphragm photometer, with a cooled Burle C31034 photomultiplier and a set of five filters U , B , V , R_C , I_C were used. Their response curves were close to the standard Johnson–Cousins $UBV(RI)_C$ system (Table 1). Additionally, two intermediate–band interference filters ($FWHM \approx 100\text{\AA}$), "h" (located at H_β around $\lambda = 4870\text{\AA}$) and "c" (located in the continuum around $\lambda = 4804 \text{ \AA}$) were used. The accuracy of these measurements was

± 0.028 , ± 0.021 , ± 0.018 , ± 0.017 and ± 0.021 in $UBVR_CI_C$ respectively. Data around the last 2006 secondary minimum have been obtained with two new CCD detectors (SBIG: STL 11000 and STL 1001) with new filters set. The mean wavelength of these photometric systems are presented and compared with the two previous photometric systems in Table 1. The accuracy was ± 0.018 , ± 0.007 , ± 0.005 , ± 0.007 and ± 0.008 in $UBVR_CI_C$ filters respectively. HD 258848 was chosen as a comparison star and GSC 1332:0578 as a check star, both suggested by Terrell *et al.*¹¹. Our original differential magnitudes ($OWGem - HD258848$) are presented in the Appendix (Tables 8,9, 10,11), and as $UBVRI$ light curves in Figure 1.

Table 1: Mean wavelength of the four photometric systems used by us.

receiver:	EMI 9558B	Burle C31034	SBIG:STL 11000	SBIG:STL 1001
band	$\bar{\lambda}[\text{\AA}]$	$\bar{\lambda}[\text{\AA}]$	$\bar{\lambda}[\text{\AA}]$	$\bar{\lambda}[\text{\AA}]$
U	3708	3678	3676	~ 3600
B	4342	4467	4392	~ 4400
V	5436	5426	5343	5404
R	6391	6689	6319	6414
I	7420	8380	8020	8305

Period analysis

The O-C analysis was carried out for verification of the orbital period and for determination of the time between primary and secondary minima. The times of minima from our observations and the time of the secondary minimum from Williams² were obtained using Kwee and Van Woerden method¹². The times of collected minima are presented in Table 2. The moment of primary minimum with $E = 18$ was excluded from the analysis because of its obviously high error. The values of O-C residuals for the primary events were calculated from Williams & Kaiser's⁴ ephemeris:

$$JD_{minI} = 2415779.0(\pm 0.4) + 1258.59(\pm 0.03) \times E, \quad (1)$$

and are shown in Figure 2. The best fit to these data gives the new ephemeris:

$$JD_{minI} = 2415778.98(\pm 0.22) + 1258.580(\pm 0.011) \times E \quad (2)$$

Table 2: The moments of primary and secondary eclipses of OW Gem used for O-C analysis. The values of O-C for the primary were derived using equation 1, and for the secondary with the adopted initial value of the phase shift $\Delta\phi_{II} = 0.23$.

E	JD-2400000	error	O-C	Author	Ref
Primary					
0	15779.4	—	0.400	Kaiser	4
2	18295.8	—	-0.380	"	4
4	20812.5	—	-0.860	"	4
5	22072.5	—	0.550	"	4
9	27105.6	—	-0.710	"	4
9	27106.9	—	0.590	"	4
15	34658.0	—	0.150	Fuhrmann	4
16	35916.0	—	-0.440	"	4
18	38435.0*	—	-1.380*	"	4
25	47243.4	± 0.5	-0.350	Kaiser <i>et al.</i>	4
26	48502.1	± 0.4	-0.240	Williams & Kaiser	4
27	49760.857	± 0.052	-0.073	Hager	13
27	49760.68	± 0.03	-0.250	this work	—
27	49760.59	± 0.02	-0.340	Kaiser <i>et al.</i>	9
29	52277.77	± 0.01	-0.340	Kaiser <i>et al.</i>	9
29	52277.73	± 0.2	-0.380	Derekas <i>et al.</i>	7
Secondary					
25	47535.50	± 0.91	2.547	Williams	2
27	50053.84	± 0.71	3.727	this work	—
27	50053.2	± 0.2	3.087	Kaiser <i>et al.</i>	9
29	52570.9	± 0.1	3.627	Kaiser <i>et al.</i>	9
29	52570.30	± 0.13	3.027	this work	—
30	53829.32	± 0.20	3.467	this work	—

* - excluded from our analysis

The values O-C for the secondary minima were calculated assuming a new period $P=1258.58$ days (Equation 2) and taking into account an initial value of the phase shift $\Delta\phi_{II} = 0.23$ according to Williams² which corresponds to 289.473 days (Figure 2). The residuals obtained for the six measured secondary minima give a mean value $\overline{O-C}=3.25 \pm 0.19$ days and hence the new phase shift is $\Delta\phi_{II} = 0.23258 \pm 0.00016$.

Preparation of photometric data

We have used five sets of photometric data for modelling. Four sets were obtained in Piwnice Observatory, two with photomultiplier detectors and two with CCDs. The fifth set of CCD data were obtained by Derekas *et al.*⁷. They reported a possible existence of asymmetry in the light curve of the primary eclipse. This effect is not visible in any other data. It seems to be an artefact. Figure 1 in Derekas *et al.*⁷ paper shows that all of the $VR_C I_C$ Szeged Observatory data points lie somewhat above the fit to Piszkéstető Observatory data points. Because of this we used only Piszkéstető data to improve the primary eclipse time covering. As a consequence we have collected data from five different photometric systems, which are somewhat shifted in magnitude. Additionally, the depth of minima in particular bands depends on their mean wavelengths. The correction for the depth of secondary eclipse is very small in respect to primary eclipse. To transform the data to the homogenous systems without correction for depth of primary eclipse, we shifted the BVR_C Piszkéstető CCD data (the star GSC 1332-0578 was the comparison star for this data), and UBVR Toruń data obtained with Burle C31034 photomultiplier and STL CCDs to the data obtained in 1995 with EMI 9558B photomultiplier (Table 1). The I passband established by EMI 9558B photomultiplier differs considerably from both Johnsons I and Cousins I_C , so the I passband data obtained in the region of phase of primary eclipse were excluded from analysis. The I passband established by STL 1001 CCD detector is quite close to the Cousins I_C passband, so this system was adopted as the reference system for the infrared domain. The magnitudes from transformed systems were shifted on reference systems by values presented in Table 3.

Table 3: Values of shifts from transformed systems on reference systems.

	Ref.syst. EMI9558B				Ref.syst. STL1001
	<i>U</i>	<i>B</i>	<i>V</i>	<i>R</i>	<i>I</i>
Trans.syst.					
EMI9558B	–	–	–	–	–0.134
Burle C31034	–0.036	+0.052	–0.008	+0.076	+0.015
STL 11000	+0.128	+0.044	–0.041	–0.014	–0.041
STL 1001	+0.137	+0.062	–0.005	+0.013	–
Piszkéstető	–	+0.979	+0.891	+0.860	–

Additionally, the depths of the secondary minima in transformed systems were corrected on reference systems according to expresion:

$$m_{ref.} = \bar{m}_{ref.} + (m_{trans.} - \bar{m}_{trans.}) \times \alpha_{ref./trans.} \quad (3)$$

where individual values of measured brightnesses are denoted by m , mean brightnesses outside of eclipses by \bar{m} (see Table 4), and the α parameter is ratio of the depth minimum in reference systems to the depth minimum in transformed systems (see Table 5).

Table 4: Mean differential magnitude (OW Gem - HD 258848) outside the eclipses in particular photometric systems.

	<i>U</i>	<i>B</i>	<i>V</i>	<i>R</i>	<i>I</i>
EMI9558B	-0.002	-0.336	-0.762	-1.020	-1.241
Burle C31034	0.034	-0.388	-0.754	-1.096	-1.390
STL 11000	-0.130	-0.380	-0.721	-1.006	-1.334
STL 1001	-0.139	-0.398	-0.757	-1.033	-1.375

Values of the α parameter were obtained by fitting a 2nd order polynomial $Depth(\bar{\lambda})$ to the observational depths of the secondary eclipse data obtained with the Burle C31034 photomultiplier. All the brightnesses were normalized to unity corresponding to the mean magnitudes outside the eclipse (Table 4) as it is needed by the differential correction (DC) procedure of the Wilson – Devinney code.

Table 5: Ratio ($\alpha_{ref./trans.}$) of the depth secondary minima in reference systems to the depth secondary minima in transformed systems.

$\alpha_{ref./trans.}$	<i>U</i>	<i>B</i>	<i>V</i>	<i>R</i>	$\alpha_{ref./trans.}$	<i>I</i>
$\alpha_{EMI9558B/BurleC31034}$	1.019	0.951	1.002	0.954	$\alpha_{STL1001/EMI9558B}$	1.087
$\alpha_{EMI9558B/STL1001}$	1.020	0.980	1.009	0.996	$\alpha_{STL1001/BurleC31034}$	0.994

Modelling the system parameters - methods of solution

We have calculated a simultaneous solution to the photometric data described above and the velocity curves. We have used both the DC and light and velocity curve (LC) programs of the 2003 version of the Wilson – Devinney code^{14,15}, where the radiative functions used are based on Kurucz’s stellar atmosphere models. This allows us to model giants or supergiants in addition to main sequence stars. So, the use of this version of the WD program is more suitable in the OW Gem case. On the other hand in the 2003 version the previous effective wavelength characterization of the bandpasses was

replaced by integration over the actual bandpasses of the standard photometric systems. Twenty five standard bands are available in the code. Five of our bands $UBVRI$ used in the analyses adjust well for the $UBVR_CI_C$ standard bands defined in the program. Unfortunately, our h, c bands do not have equivalents among the standard ones, so we decided to omit them in our analyses.

The Levenberg – Marquardt's algorithm used in the 2003 version of the WD program together with a properly selected value of the λ parameter (see e.g. Kallrath & Milone¹⁶; Kallrath *et al.*¹⁷) usually allows finding a solution in the parameter space even when a large group of free parameters for simultaneous iterations is used. However, the OW Gem orbit is characterized by strong eccentricity which amplified correlations between the parameters. We have used the method of multiple subsets (MMS) recommended by Wilson & Bierman¹⁸ for dealing with this problem. The method relies on disposing the strongest correlation through separation of the most correlated parameters into different groups. In our case the groups have included two (seldom three) weakly correlated parameters. The use of the method does not significantly extend the time of calculation, but a problem appears in the form of unrealistically small values of the errors. We have received more plausible values of errors by executing additional iterations with all the free parameters simultaneously. The solution was calculated with the aid of a program we wrote for "semiautomatic" iteration, which made it possible to keep control over the result of each iteration by visual inspection of the evolution of parameters, errors and residuals on the computer screen as a function of the iteration number. The criterion for a proper solution was set as obtaining the minimum sum of squared residuals over the domain of parameter space as well as (in some cases) visual inspections of the shape of the χ^2 surface.

Fixed parameters

OW Gem photometric behaviour does not indicate the possibility of the occurrence of spots on the component's surface, so the system was treated as not spotted. Synchronous rotation has been assumed. It is impossible to find out the temperatures of both the components in OW Gem case using only the WD code, so the temperature T_1 of the hot component was fixed at $7100K$ according to the $F2Ib - II$ classification⁵. The values of both stars' temperatures are below $7200 K$, which is a theoretical upper threshold for convective envelopes. Such cases are characterized by the theoretical values of a bolometric albedo $A = 0.5$ and the exponent in the bolometric gravity brightening $g = 0.32$ (Lucy¹⁹). The third light contribution has been neglected. The derivatives of the orbital period and ω were assumed to be equal to zero. A nonlinear, logarithmic limb darkening law was used. The theoretical coefficients x, y have been calculated accord-

ing to the Van Hamme²⁰ tables for: $T_1 = 7100K$, $T_2 = 4950K$, $\log g_1 = 2.2$, $\log g_2 = 2.0$.

The free parameters' initial values

The initial values of $a \sin i = 1052R_{\odot}$, $V_{\gamma} = -5.25kms^{-1}$ and $q = M_2M_1^{-1} = 0.676$ have been adopted from Griffin & Duquennoy⁵. The values of the surface linear potentials of the stars were initially estimated as $\Omega_1 = 35$, $\Omega_2 = 24$ from the value of the radius $R_1 = 30R_{\odot}$, $R_2 = 35R_{\odot}$, and mass ratio. A temperature $T_2 = 4950K$ and an inclination $i = 89^{\circ}$ have been taken from our simple model¹⁰. The large orbital eccentricity enables to estimation of the parameters e and ω when we have information about the time separation of the eclipses and about the duration of the phenomena. From there we have found the initial values of $e = 0.5183$ and $\omega = 144.04^{\circ}$ using formulae 4.4.60 and 4.4.61 from Kallrath & Milone¹⁶. The parameter ϕ_0 was treated differently. This parameter is connected with manner of orbit solution and it is only formal parameter of WD code, where for circular orbits phase of periastron is equal to 0.0 for $\omega = 90^{\circ}$ by definition. If we want to get actual value of periastron phase with WD code for eccentric orbit we have to take into account the value of phase correction ϕ_0 . This parameter can be briefly defined as difference of actual periastron phase for eccentric orbit and periastron phase that would be for circular orbit with adopted the same periastron longitude ω . Three parameters: eccentricity e , periastron longitude ω and ϕ_0 parameter are each other dependent. For that reason parameter ϕ_0 can not be treated directly as the other free parameters, but it have to be searched through the wide area of this parameter's space in order to find the global minimum and not to land in a local one.

The orbital geometry solution

The solution was carried out in two basic steps. Both stages of calculations were carried out for many values of ϕ_0 parameter according to described below procedure. The first stage aimed to determine the geometry of the orbit through estimation of the parameters: $a \sin i$, e , ω , V_{γ} , q and L_1 . The bandpass luminosity L_1 of the primary component is defined in details in the manual of the 2003 version of the WD program. The changes in two parameters, the argument of the periastron ω and the eccentricity e , have a strong influence on the light curves as well as on the velocity curves. The duration of both eclipses and their phase shift depend very strongly on the variations of these two parameters. This timing puts a strong limitation on the values e and ω . The WD program enables solving both velocity curves and many light curves simultaneously²¹. This advantage of WD code has been used in the first part of the first stage, where the values of the parameters e , ω , L_1 were corrected. When a convergence was achieved,

then in the second part of the first stage, the parameters $a \sin i$, V_γ , q , which depend only on velocity curves were corrected, then both steps were repeated. The second stage had the purpose of determining first of all the orbital inclination i together with the other parameters depending only on the light curves: T_2 , Ω_1 , Ω_2 , L_1 . Ω_1 and Ω_2 are linear functions of the true potentials on the equipotential surfaces of the stars¹⁴. A black–body approximation was used. In order to make the geometric solutions independent of the input values of the radii and the inclination, the first stage of the solution (searching for $a \sin i$, e , ω , V_γ , q) has been repeated again. A further repeating of both stages did not show changes in the errors limits, so it was considered that for the current value of ϕ_0 parameter the final solution for the orbital parameters has been achieved. Each value of ϕ_0 parameter relate to one value of sum of weighted squared residuals ($\chi^2 = \Sigma(W \cdot Res^2)$), which constitute the quality of obtained fit. The second order polynomial was fitted for $\chi^2(\phi_0)$ function and the minimum of the function was found (Figure 3). This way the final set of orbital parameters has been found and these values are compared with previous solutions in Table 6. The radial velocity curves computed from our parameters (Figure 4) differ slightly from those published earlier by Griffin & Duquennoy⁵ and Terrell *et al.*⁸. A good timing of both minima gives better values for ω and e in comparison to previous solutions. However, these parameters force small changes in $a \sin i$, V_γ and q in comparison to the free fitting.

Table 6: Orbital parameters of OW Gem.

	This work	Griffin 2007**	Terrell <i>et al.</i> ⁸	G&D ⁵	unit
P	1258.58	1259.30	1258.59	1260.00	day
$a \sin i$	1030.0 ± 10.0	1035.9 ± 11.8	1044.4 ± 8.8	1052.0 ± 18.7	R_\odot
i	89.040 ± 0.028	–	89.09 ± 0.02	89.0 ± 0.1	degree
V_γ	-5.10 ± 0.10	-5.21 ± 0.06	-5.18 ± 0.14	-5.25 ± 0.16	kms^{-1}
q	0.692 ± 0.011	0.687 ± 0.013	0.664 ± 0.002	0.676 ± 0.014	–
e	0.5286 ± 0.0006	0.5233 ± 0.028	0.51718 ± 0.00002	0.515 ± 0.011	–
ω	140.73 ± 0.12	140.3 ± 0.5	143.08 ± 0.02	140.2 ± 1.3	degree
ϕ_0	-0.1004 ± 0.0001	–	-0.1030 ± 0.0001	–	–
$\Delta\phi_{II}$	0.23250	0.23655	0.23207	0.24123	–
$\delta\phi_{II}^*$	+0.10	-5.00	+0.64	-10.89	day

* - The differences between the observed and calculated phase shift of the secondary eclipse

** - Private communication

The final solution must give a formally larger standard deviation of the observational points than a free fitting to the radial velocities only, without any timing constraints. This is in contradiction to the Terrell *et al.*⁸ solution, who obtained unrealistically low errors for e and ω , as commented by Griffin²². Moreover, a detailed inspection

of "Figure 1" in Terrell *et al.*⁸ shows, that almost all the points which lie on the descending branch of the secondary minimum are above their synthetic light curves while, the points which lie on the ascending branch are located below their model. This disagreement in the timing has been previously noted by Griffin²². Values e and ω parameters obtained by Terrell *et al.*⁸ differ significantly from the others results and we have found that their solutions must landed in the local minimum as a consequence of use incorrect ϕ_0 value. Values e and ω parameters which Griffin (2007, private communication) has obtained with his own, new radial velocity (Appendix – Table 12) are close and almost consistent in borders of errors to our values. However, because of lack of photometry in those solution it is not proper pair of values, and such e and ω parameters can not give a good timing of the secondary minimum. The differences between the observed phase shift of the secondary eclipse $\Delta\phi_{II} = 0.23258$ and that derived from the orbital solution (Table 6) are +2.4 hours for our solution, +15.4 hours for Terrell *et al.*⁸ and minus a few days for orbital parameters carried out from radial velocity only. Taking into account that we have obtained such a good timing from our analysis, we hope that our parameters are close to the true ones with realistic errors.

System components physical parameters solution

Knowledge about the orbital geometry allows us to proceed with a part of the modelling leading to exact information about the physical parameters of the components, i.e. temperatures, radii, masses, luminosities. At this stage of the solution a stellar atmospheres approach has replaced the previous black-body approximation. The temperature of the hot component have to be adopted. It is not possible to determine temperature of the both OW Gem components if we do not have at disposal very good quality photometry (accuracy better than $0.^m01$) of both eclipses reaching deep UV and far infrared domain. We have not, and we can obtain temperatures ratio only. The Griffin & Duquennoy⁵ have classified the hot component spectral class as $F2Ib - II$, that according to Straižys & Kuriliene²³ spectral class - effective temperature classification gives value of temperature $T_1 = 7100K$. This value of hot component temperture was adopted in our calculations, the same as in other papers. However, we have compared of the OW Gem spectrum with spectra of neighbour class standards, and we have found that the accuracy of this classification is of the order of one subclass. By interpolations with Straižys & Kuriliene²³ spectral class - effective temperature classification we have estimated uncertainty for temperature of hot component $T_1 = 7100^{+150}_{-200}K$ and for corresponding temperature of cold component via temperature ratio as $T_2 = 4975^{+110}_{-140}K$ (see table 7). The error of our T_2 value given in table 7 it is error of fit to observational data and not the error of parameter determination.

The orbital inclination and radius of the primary component R_1 have been found by a search of the "whole" χ^2 surface for their possible values. The method relies on the execution of many fits where the two wanted parameters are fixed and they are changed in the next runs with the assigned resolution. Such a map of the χ^2 function usually allows to find a global minimum, and so proper values of the parameters. The surface $\chi^2(i, R_1)$ has been obtained by calculating a grid of 130 values of χ^2 (Figure 5), for which a 3th order polynomial $f(x, y)$ was fitted. Later on, the minimum of the function $f(x, y)$ was found. In this way, the inclination i and the radius of primary component R_1 have been determined, and respondent the values of the radius of secondary componenet R_2 , temperature T_2 and the luminosity L_1 . The resulted value of the inclination is shown in the Table 6. Table 7 presents our physical parameters in comparison to those of other authors. Figure 6 demonstrates the quality of the fit to U and V light curves, and Figure 7 demonstrates the variations in the $B-R$ color index during the primary and the secondary eclipses of OW Gem.

Table 7: A comparison of the physical parameters obtained by us, Terrell *et al.* and Griffin & Duquennoy.

	This work	Terrell <i>et al.</i> ⁸	G&D ⁵	unit
T_1^*	7100	7100	7100	K
T_2	4975 ± 20	4917 ± 110	4800	K
Ω_1	33.34 ± 0.21	35.15 ± 0.03	–	–
Ω_2	24.17 ± 0.15	24.19 ± 0.01	–	–
R_1	32.32 ± 0.22	30.9 ± 0.3	30 ± 3	R_\odot
R_2	32.56 ± 0.23	31.7 ± 0.3	35 ± 3	R_\odot
M_1	5.49 ± 0.21	5.8 ± 0.2	5.9 ± 0.3	M_\odot
M_2	3.80 ± 0.16	3.9 ± 0.1	4.0 ± 0.2	M_\odot
$(L_1/(L_1 + L_2))_U$	0.949 ± 0.011	0.946 ± 0.008	0.945	–
$(L_1/(L_1 + L_2))_B$	0.921 ± 0.007	0.924 ± 0.005	0.899	–
$(L_1/(L_1 + L_2))_V$	0.851 ± 0.007	0.868 ± 0.006	0.834	–
$(L_1/(L_1 + L_2))_R$	0.803 ± 0.008	0.815 ± 0.004	–	–
$(L_1/(L_1 + L_2))_I$	0.757 ± 0.009	0.761 ± 0.005	–	–
★ - adopted				

OW Gem spectrum

We used the coude-spectrograph of the 2m RCC telescope at the Rozhen Observatory (Bulgaria) to obtain spectra of OW Gem, with a resolving power $R \sim 15000$, on January 20, 2005 ($\phi \sim 0.88$) and April 14, 2006 ($\phi \sim 0.24$). The spectral regions covered

were 6620-6825 Å and 6470-6820 Å respectively. In Figure 8 the spectra of OW Gem are compared with spectra of HD 164136 (*F2II*), HD 75276 (*F2Iab*) and HD 159532 (*F1II*). The spectrum of HD 164136 (ν Her) is from the Indo-U.S. library of coudé feed stellar spectra (Valdes *et al.*²⁴) and the spectra of HD 75276 and HD 159532 are from the UVES library of high-resolution spectra (Bagnulo *et al.*²⁵). Additionally, a spectrum of the possible merger V838 Mon (Tylenda & Soker²⁶, and references therein), obtained at the Rozhen Observatory with the same resolution as the OW Gem spectra, is shown in Figure 8 as well.

In the both spectra the radial velocities were measured (Table 13). In the spectrum on April 14, 2006, obtained during the secondary eclipse, we measured the radial velocity of the primary component only.

Griffin & Duquennoy⁵ classified the primary component of OW Gem as an *F2Ib-II* star. We do not have enough spectral observations and intention to make a detailed spectral classification of both components. However, in Figure 8 it is obvious that the lines in the OW Gem spectrum on April 14, 2006 dominated by the primary component are very similar to the ones in the *F2Iab* spectrum of HD 75276. The most remarkable difference between the spectrum of the OW Gem primary and the spectra of ν Her (noted by Griffin & Duquennoy⁵) and HD 159532 is the rotational velocity which is $V \sin i = 28 \text{ km s}^{-1}$ for ν Her and $V \sin i = 105 \text{ km s}^{-1}$ for HD 159532 (Snow *et al.*²⁷). Based on the January 20, 2005 spectrum only, we cannot say anything about the secondary companion spectral class.

The above spectral regions were chosen with the aim of checking up the presence of a weak Li I 6708 Å line in the spectrum of the secondary component suggested by Griffin & Duquennoy⁵. These authors measured an equivalent width of about 10 or 15 mÅ for this lithium line in the composite spectrum. Our April 14, 2006 spectrum (just during the secondary eclipse) is dominated by the primary component. If the lithium line is present then it should be detectable in the January 20, 2005 spectrum (about 5 months before the primary eclipse) in which most of the absorptions are double because of the blending of both component lines. The quality of our spectra is good enough to identify and measure such weak absorptions. As can be seen in Figure 8, in both spectra there are several faint features with equivalent widths of the order of 10-15 mÅ in the vicinity of the lithium line. On one hand, none of these faint features disappear in the spectrum on April 14, 2006, as we would expect if the weak lithium line were present only in the secondary spectrum. On the other hand, the radial velocity measurements show that all of these faint features are far from the expected lithium line position for both stars. Therefore, we cannot confirm the presence of the Li I 6708 Å absorption line, neither in the primary component spectrum nor in the secondary component spectrum.

To explain the unusual evolutionary status of the components, Eggleton²⁸ suggested that OW Gem is a former triple star in which the F supergiant is a merged remnant of a close sub-binary. He pointed out that it is very difficult to confirm that a particular star is or is not the result of a merger. A merger remnant could be an unusually rapidly rotating star (Eggleton²⁸) but it is obvious from Figure 8 that this is not the case of the OW Gem primary component. After the merging, a relatively strong Li I 6708 Å absorption line is present in the spectrum of V838 Mon (Figure 8). As was noted above, this line is missing in the spectrum of the OW Gem primary component. Hence, we can consider the slow rotation and the lithium line absence only as an indication that, in case the primary component in OW Gem is a merger remnant, the merger event took place a long time ago.

Conclusions

The full set of orbital and physical parameters for OW Gem have been obtained with independently collected photometric data. A slightly better values pair's of parameters $\omega = 140^\circ.73$ and $e = 0.5286$ was obtained in our work in comparison to the previous analysis. Both the eccentricity and the periastron argument calculated in this paper give a better fit to the observations, especially to the best timing of the secondary minimum. This was possible by using new data including three secondary minima. Our results underline the advantage of the simultaneous analysis of light and velocity curves. The new model have supplied a better estimate of the radii of the OW Gem components, using good quality multicolour photometry as well as more reliable temperature ratios of the stars. However, we were not able to significantly change the values of the masses and the mass ratio of the components, confirming once again the unclear evolutionary status of the system, in which two massive stars with considerably different masses ($\sim 6M_\odot$ and $\sim 4M_\odot$) are placed in a very short stage of evolution of the supergiants. A confrontation with the solar metallicity evolutionary tracks from Girardi et al.²⁹ is presented in Figure 9. The less massive star is about 200 million years old. The more massive star is at least 100 million year evolutionary younger. During this time it should finish its evolution as a supergiant. The current evolutionary status of the system stands in contradiction with evolutionary models of the stars in binary systems and cannot be explained either by loss or by transfer of mass (Griffin & Duquennoy⁵). In order to explain the observed parameters of OW Gem, we should revise the stellar evolution theory. Another possibility is that a merger took place. Eggleton²⁸ suggested that a triple system (close sub-binary $4M_\odot + 2M_\odot$ with short period about 2^d and the third component $4M_\odot$ on wide orbit) can turn into a binary system. The lack of lithium line detection in the present spectra is an indication that the merger event would have had

to have taken place long time ago.

It seems that future attempts of modelling optical light and velocity curves will not result in significant changes in our knowledge about the physical parameters of the system. Nevertheless, the OW Geminorum case still remains unexplained and an important case for understanding the evolution of the binary stars. Especially the depths of the primary and secondary eclipses in deep UV and far infrared can give the best, direct calibration of surface temperature for F and G supergiants. In present times it has became possible to obtain an angular separation of such a few (about 3) milliarcseconds separated binary star by optical interferometric observations (see e.g. Konacki & Lane³⁰), and it gives opportunity for verification of the distance to the OW Gem system.

Acknowledgements

We specially thank to Dr R.F. Griffin, who together with Dr A. Duquennoy have discovered unusually interesting nature of OW Gem system, for his permission to use of the radial velocity data collected by them since their paper in 1993. We are also deeply grateful to him for helpfull and kindness discussion. We are very grateful to Dr B. Roukema for his language corrections and for N. Biernaczyk, S. Frąckowiak, P. Oster, K. Rumiński, E. Świerczyński, M. Więcek, P. Wirkus, K. Wojtkowska, M. Wojtkowski, P. Wychudzki for their contribution to collection of photometric data. This study was supported by MNiSW grant No. N203 018 32/2338, grant UMK No. 340-A, and partly supported by the Polish–Bulgarian Academy of Sciences exchange.

References

- (1.) D. H. Kaiser, M. E. Baldwin, D. B. Williams, D.B., *Inf. Bull. Var. Stars*, no. 3196, 1988.
- (2.) D. B. Williams, 1989, *J.A.A.V.S.O.*, **18**, 7, 1989.
- (3.) D. H. Kaiser, *Inf. Bull. Var. Stars*, No. 3233, 1988.
- (4.) D. B. Williams, & D. H. Kaiser, *J.A.A.V.S.O.*, **20**, 231, 1991.
- (5.) R. F. Griffin, & A. Duquennoy, *The Observatory*, **113**, 53, 1993.
- (6.) R. F. Griffin, *The Observatory*, **113**, 294, 1993.
- (7.) A. Derekas, *et al.*, *Inf. Bull. Var. Stars*, no. 5239, 2002.
- (8.) D. Terrell, *et al.*, *A.J.*, **126**, 902, 2003.
- (9.) D. H. Kaiser, *et al.*, *Inf. Bull. Var. Stars*, no. 5347, 2002.
- (10.) M. Mikołajewski, C. Gałan, D. Graczyk, *Inf. Bull. Var. Stars*, no. 5445, 2003
- (11.) D. Terrell, D. H. Kaiser, D. B. Williams, *Inf. Bull. Var. Stars*, no. 4102, 1994.
- (12.) K. K. Kwee, & H. Van Woerden, *Bull. Astron. Inst. Netherlands*, **12**, 327, 1956.
- (13.) T. Hager, *J.A.A.V.S.O.*, **24**, 9, 1996.

- (14.) R. E. Wilson, & E. J. Devinney, *Ap.J.*, **166**, 605, 1971.
- (15.) R. E. Wilson, *Ap.J.*, **356**, 613, 1990.
- (16.) J. Kallrath, & E. F. Milone, *Eclipsing Binary Stars: Modeling and Analysis*, (New York: Springer), chap.4., 1998.
- (17.) J. Kallrath, *et al.*, *Ap.J.*, **508**, 308, 1998.
- (18.) R. E. Wilson, & P. Biermann, *A.&A.*, **48**, 349, 1976.
- (19.) L. B. Lucy, 1967, *Z. Astrophys.*, **65**, 89, 1967.
- (20.) W. Van Hamme, *A.J.*, **106**, 2096, 1993.
- (21.) R. E. Wilson, *Ap.J.*, **234**, 1054, 1979.
- (22.) R. F. Griffin, *The Observatory*, **124**, 136, 2004.
- (23.) V. Straižys, & G. Kuriliene, *Ap.&S.S.*, **80**, 353, 1981.
- (24.) F. Valdes, *et al.*, *Ap.J.S.*, **152**, 251, 2004.
- (25.) S. Bagnulo, *et al.*, *The Messenger*, **114**, 10, 2003.
- (26.) R. Tylenda, & N. Soker, *A.&A.*, **451**, 223, 2006.
- (27.) T. P. Snow, *et al.*, *Ap.J.S.*, **95**, 163, 1994.
- (28.) P. P. Eggleton, in *Exotic Stars as Challenges to Evolution*, edited by A. C. Tout & W. Van Hamme, (A.S.P. Conf. Ser. 279, San Francisco), 2002, p. 37.
- (29.) L. Girardi, *et al.*, *A.&A.*, **141**, 371, 2000.
- (30.) M. Konacki, & B. F. Lane, *Ap.J.*, **610**, 443, 2004.

Figures:

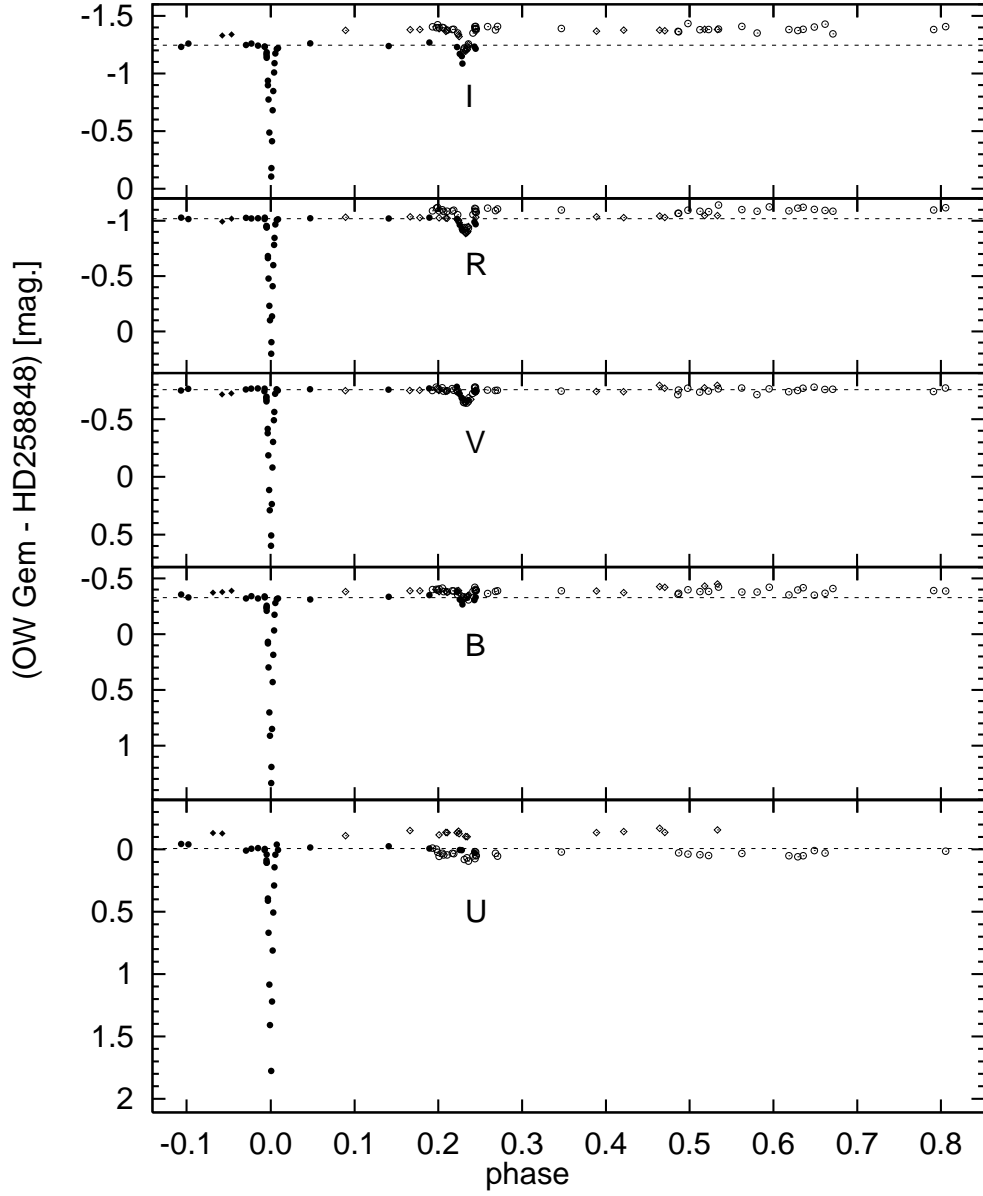


Figure 1: The *UBVRI* lights curves of OW Gem. Our original differential magnitudes are presented. The data was phased with a period of 1258.58 days. The horizontal dashed lines mark the average brightness outside of eclipse in the old photometric system with EMI 9558B photomultiplier. Data collected with photomultipliers are represented by circles, and these with CCD by diamonds. Filled symbols are used for EMI 9558B or SBIG:STL 11000 and open for Burle C31034 or SBIG:STL 1001.

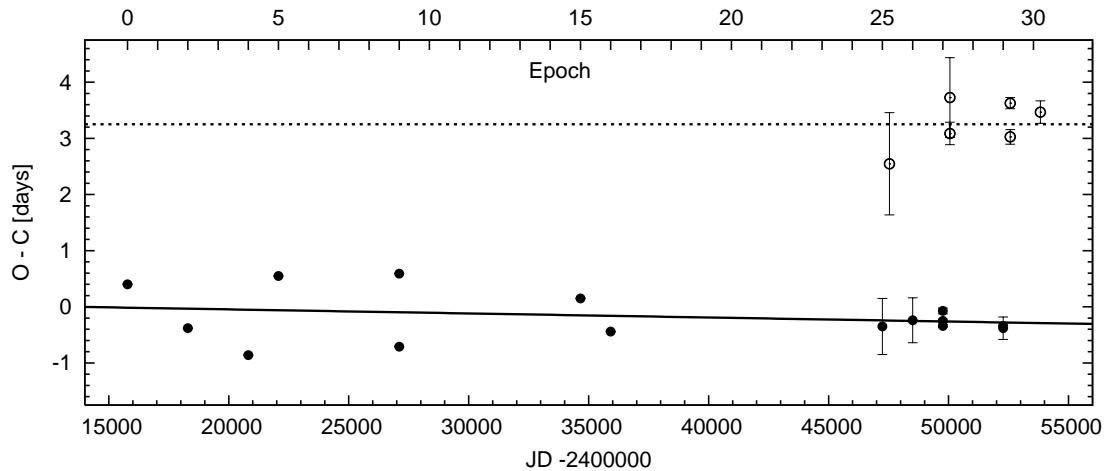


Figure 2: The O-C diagram for the moments of the primary eclipse from the ephemeris given by Equation 1 (filled circles) and the secondary eclipse from the ephemeris given by Equation 2 with phase shift adopted as $\Delta\phi_{II} = 0.23$ (open circles). The best fit for the primary eclipses (solid line) indicates a inconsiderable shorter period. The best fit for the secondary eclipses (horizontal dashed line) was found assuming the new value $P=1258.58$.

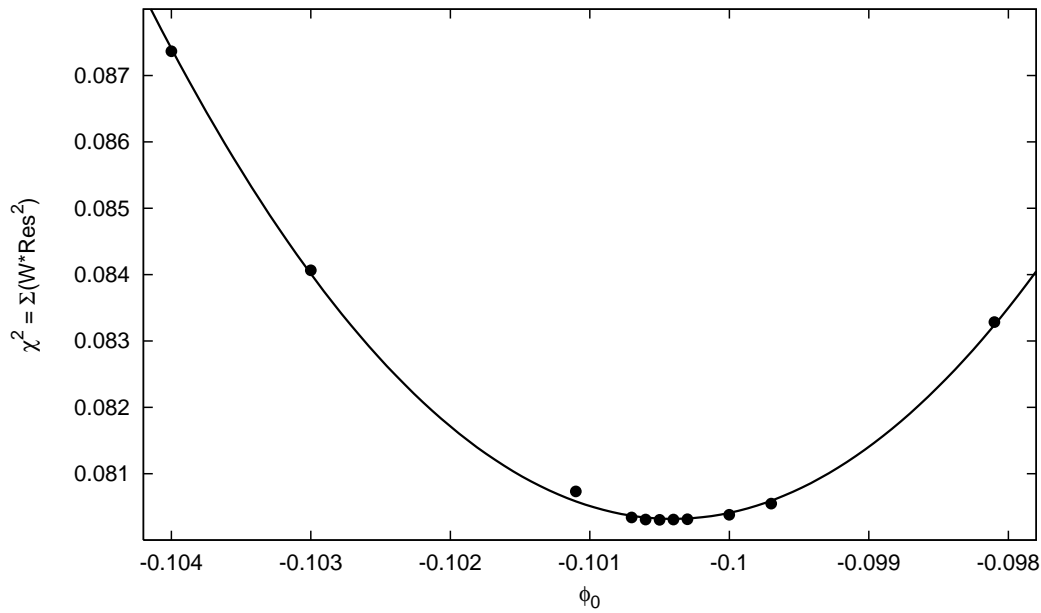


Figure 3: Quality of fit obtained for different values of ϕ_0 parameter. The polynomial $f(x)$ was fitted and the minimum of the function was found.

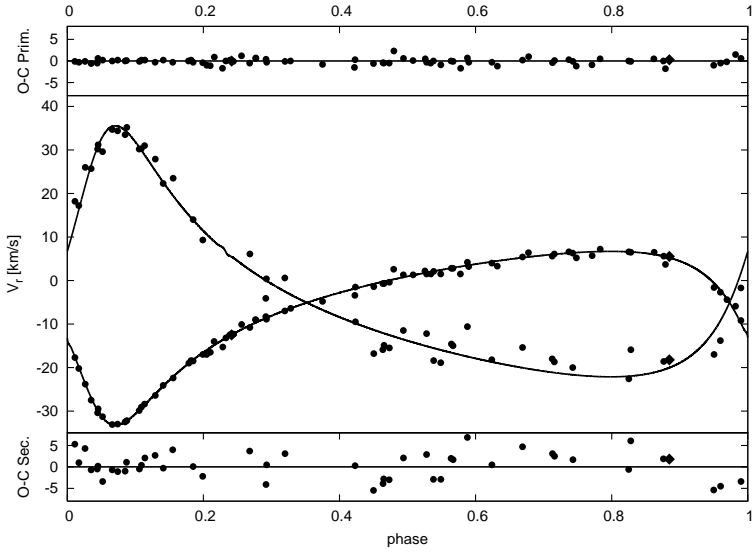


Figure 4: Synthetic radial velocity curves (lines) fitted to the Griffin & Duquennoy data represented by circles and the our three points represented by diamonds. At the top and the bottom the residuals (O-C) are placed for the primary nad the secondary components respectively, which demonstrate the quality of the fit.

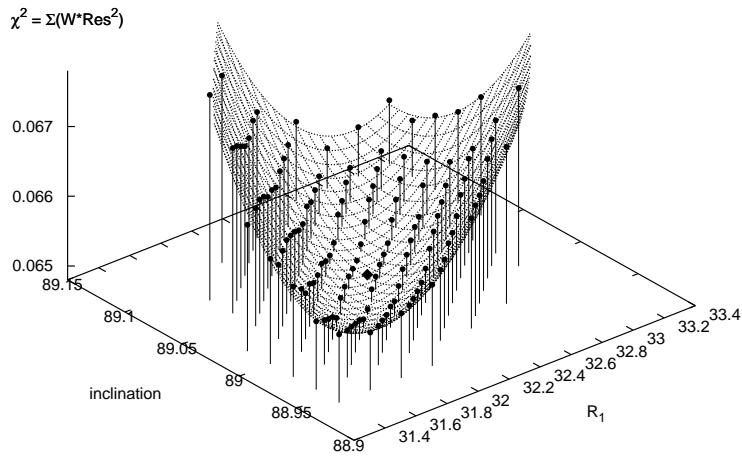


Figure 5: Adjusting of the polynomial $f(i, R_1)$ for the points on the χ^2 surface. The place of the minimum on this surface is denoted by a diamond. The radii of primary component (R_1) is expressed in solar radius units and inclination in degrees.

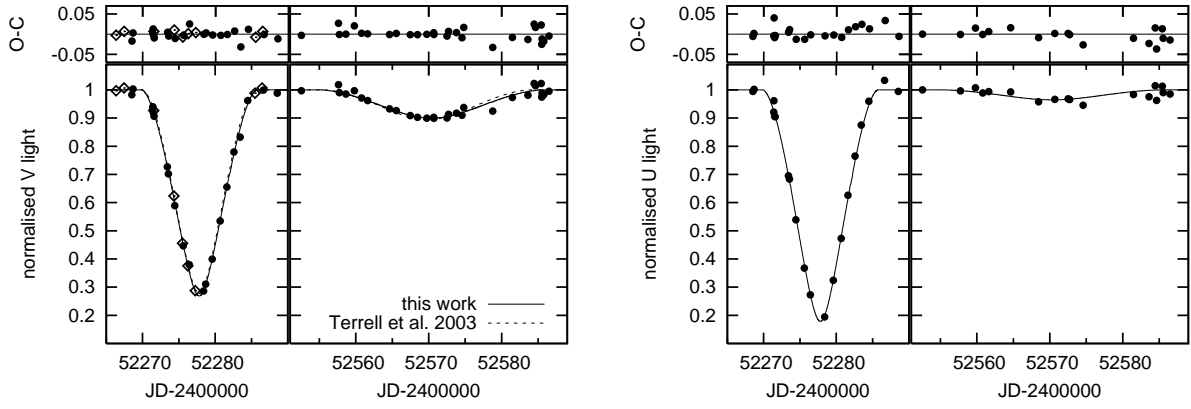


Figure 6: V (left) and U (right) light curves of OW Gem normalised to 1 out of eclipse. The filled circles represent our measurements. The Derekas *et al.*⁷ data are shown by diamonds. At the top the residuals (O-C) are placed, which demonstrate the quality of the fit. The dashed line represents the model of Terrell *et al.*⁸ where the secondary minimum is shifted about 13 hours in respect to our model (solid line).

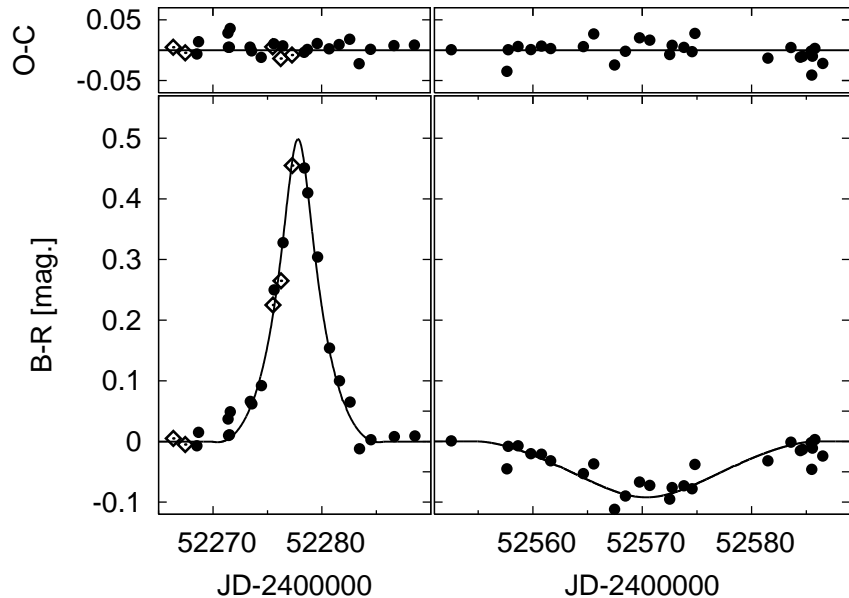


Figure 7: The $B-R$ color index during the primary and the secondary eclipses of OW Gem. The filled circles represent our measurements. The Derekas *et al.*⁷ data are shown by diamonds. At the top, the residuals (O-C) are placed, which demonstrate the quality of the fit.

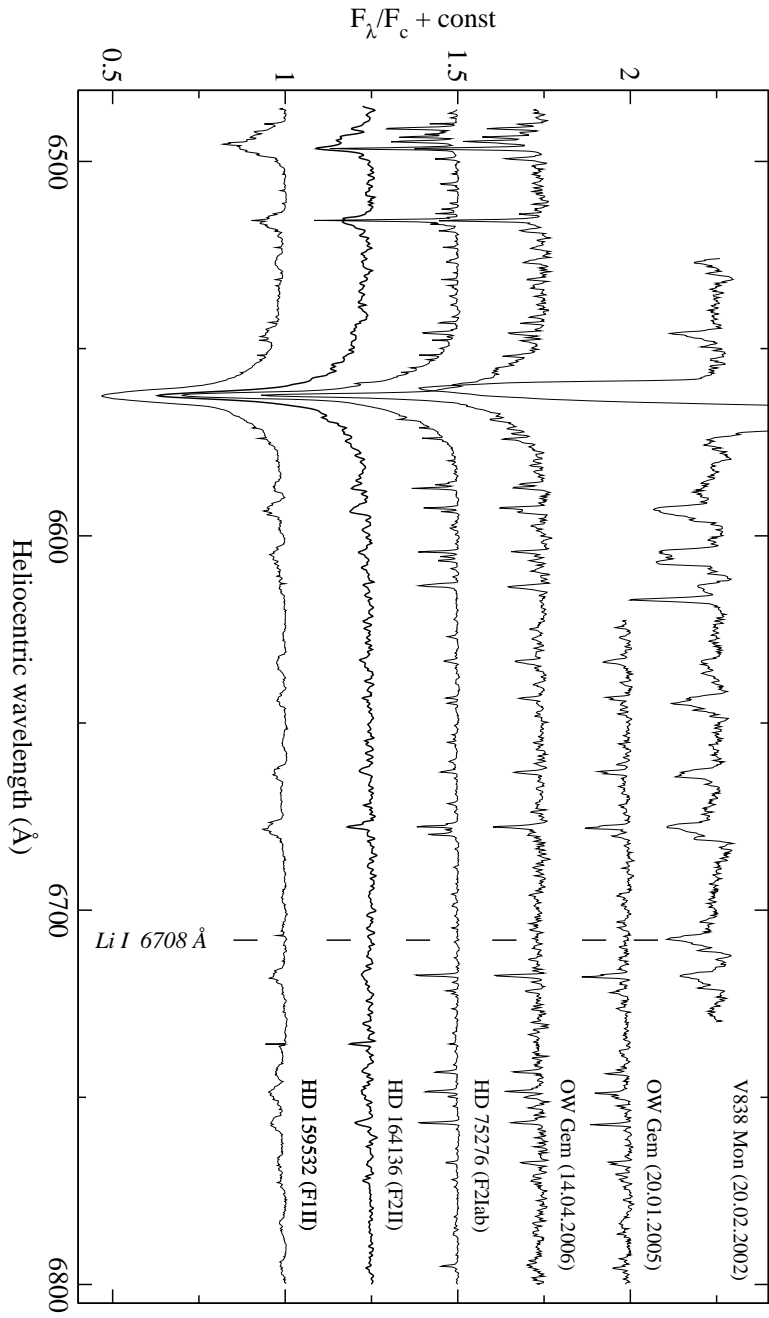


Figure 8: A comparison of our OW Gem spectra with the spectra of HD 75276, HD 164136 (ν Her), HD 159532 and the possible merger V838 Mon. The spectra of the comparison stars are shifted to the heliocentric wavelengths of the OW Gem spectra. The spectra of HD 75276 and HD 159532 are degraded to the OW Gem spectra resolution. The H_{α} emission component in the spectrum of V838 Mon is truncated for clarity.

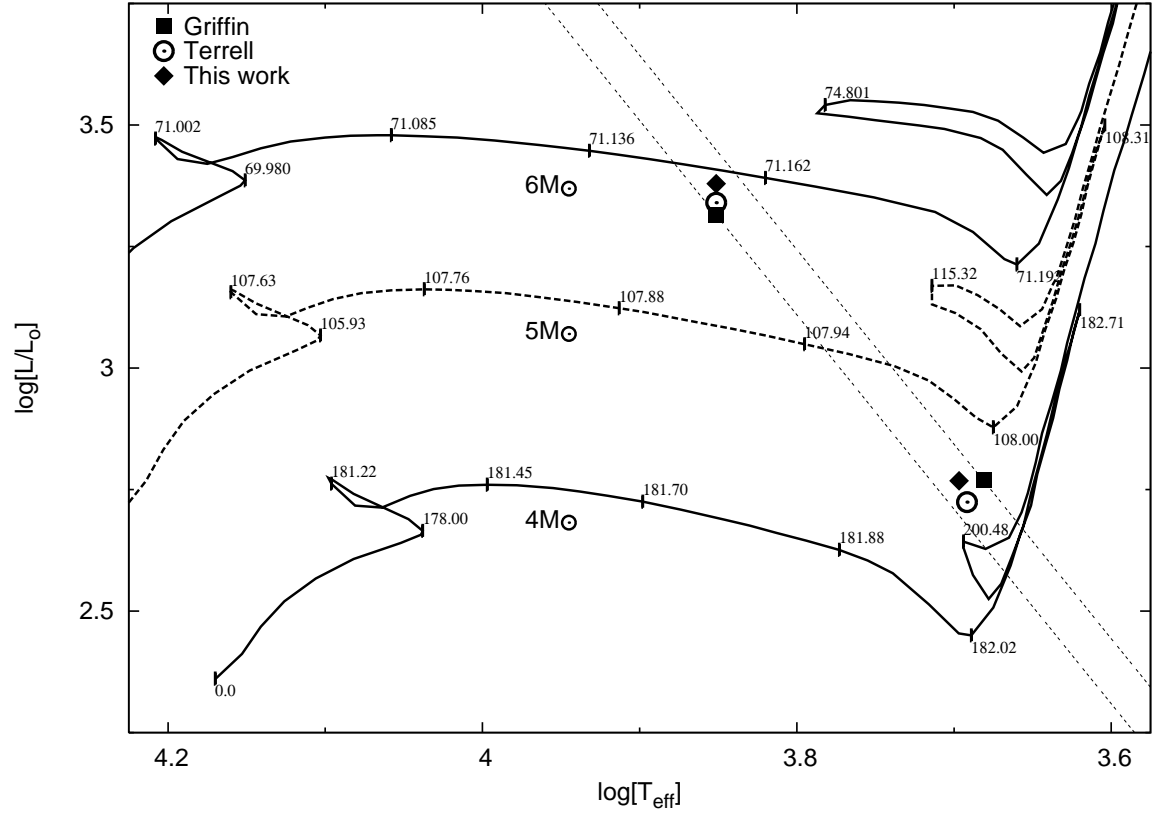


Figure 9: Both OW Gem components in confrontation with Girardi's *et al.*²⁸ solar metallicity evolutionary tracks. The diagonal dashed lines are lines of constant radius for $30 R_{\odot}$ and $35 R_{\odot}$. The evolution time in millions of years is denoted by short vertical lines with numerical value.

Appendix - photometric and radial velocity data:

Table 8: *UBVRI* light curves of the 1995 primary and secondary eclipses collected with EMI9558B photomultiplier.

$JD - 2400000$	ΔU	ΔB	ΔV	ΔR	ΔI
49723.4524	0.010	-0.320	-0.758	-1.026	-1.247
49731.3870	-0.006	-0.340	-0.766	-1.020	-1.260
49741.4052	-0.011	-0.320	-0.767	-1.022	-1.241
49751.3617	0.004	-0.339	-0.743	-1.016	-1.232
49751.5129	-0.004	-0.330	-0.765	-1.029	-1.233

$JD - 2400000$	ΔU	ΔB	ΔV	ΔR	ΔI
49754.2218	0.087	-0.233	-0.687	-0.954	-1.169
49754.2680	0.041	-0.256	-0.695	-0.950	-1.185
49754.3465	0.105	-0.243	-0.669	-0.938	-1.136
49754.4260	0.107	-0.209	-0.655	-0.942	-1.150
49756.2605	0.393	0.069	-0.416	-0.681	-0.937
49756.4032	0.411	0.084	-0.378	-0.662	-0.898
49757.2831	0.669	0.299	-0.188	-0.477	-0.774
49758.4480	1.084	0.702	0.114	-0.232	-0.488
49759.2654	1.410	0.911	0.290	-0.101	-
49761.2366	1.777	1.336	0.597	0.201	-0.106
49761.5347	-	1.191	0.507	0.097	-0.179
49762.4387	1.221	0.851	0.235	-0.137	-0.412
49763.5336	0.811	0.430	-0.082	-0.408	-0.682
49764.4510	0.507	0.185	-0.303	-0.599	-0.847
49765.4287	0.289	-0.033	-0.492	-0.782	-1.009
49766.2876	0.143	-0.174	-0.563	-0.846	-1.089
49767.3374	0.043	-0.279	-0.720	-0.966	-1.174
49769.4922	-0.038	-0.315	-0.761	-1.007	-1.214
49771.3802	0.004	-0.320	-0.749	-1.013	-1.221
50040.4597	-	-0.377	-0.782	-1.016	-1.229
50044.4597	0.005	-0.311	-0.720	-0.963	-1.171
50047.4604	0.006	-0.296	-0.686	-0.927	-1.151
50048.4013	-	-0.266	-0.679	-0.913	-1.086
50066.4347	0.025	-0.306	-0.741	-0.989	-1.232
50068.3413	-	-0.331	-0.734	-0.969	-1.215
50884.4409	-0.044	-0.355	-0.750	-1.028	-1.231
50895.3600	-0.040	-0.329	-0.764	-1.016	-1.259
51078.5412	-0.015	-0.311	-0.760	-1.022	-1.262
51196.3584	-0.025	-0.335	-0.756	-1.020	-1.239
51257.4235	-0.008	-0.350	-0.768	-1.028	-1.269

Table 9: $UBV(RI)_C hc$ light curves of the 2002 secondary eclipse collected with Burle C31034 photomultiplier.

$JD - 2400000$	ΔU	ΔB	ΔV	ΔR_C	ΔI_C	Δc	Δh
52520.5887	-0.011	-0.399	-0.750	-1.089	-1.405	-0.555	-0.605
52526.5821	-0.002	-0.401	-0.779	-1.114	-1.398	-0.549	-0.612
52528.5610	0.022	-0.395	-0.763	-1.120	-1.423	-0.569	-0.574

$JD - 2400000$	ΔU	ΔB	ΔV	ΔR_C	ΔI_C	Δc	Δh
52530.5813	0.055	-0.406	-0.761	-1.090	-1.397	-0.521	-0.626
52535.5425	0.031	-0.412	-0.772	-1.100	-1.400	-0.560	-0.578
52537.5415	0.044	-0.382	-0.745	-1.084	-1.395	-0.549	-0.562
52542.6051	0.044	-0.379	-0.748	-1.087	-1.376	-0.560	-0.565
52550.5663	0.031	-0.388	-0.765	-1.088	-1.382	-0.564	-0.589
52552.5397	0.034	-0.386	-0.751	-1.095	-1.384	-0.562	-0.596
52558.6378	-	-0.353	-0.738	-1.054	-1.351	-0.530	-0.576
52567.4629	-	-0.335	-0.650	-0.926	-1.205	-0.475	-0.505
52568.4644	0.080	-0.325	-0.643	-0.939	-1.220	-0.442	-0.510
52572.5023	0.068	-0.331	-0.640	-0.940	-1.217	-0.441	-0.490
52574.5563	0.094	-0.307	-0.652	-0.934	-1.257	-0.432	-0.431
52581.4831	0.052	-0.383	-0.724	-1.057	-1.351	-0.511	-0.577
52584.4530	0.018	-0.420	-0.778	-1.112	-1.406	-0.555	-0.605
52584.6540	0.074	-0.391	-0.770	-1.086	-1.390	-0.571	-0.579
52585.4333	0.020	-0.401	-0.778	-1.106	-1.408	-0.532	-0.578
52585.5563	0.045	-0.388	-0.741	-1.084	-1.386	-0.524	-0.574
52586.5032	0.050	-0.392	-0.749	-1.076	-1.386	-0.549	-0.543
52603.4456	-	-0.364	-0.754	-1.115	-1.406	-0.534	-0.586
52615.4383	0.031	-0.383	-0.750	-1.091	-1.378	-0.547	-0.586
52618.5081	0.054	-0.389	-0.751	-1.107	-1.408	-0.547	-0.579
52714.3303	0.021	-0.388	-0.744	-1.097	-1.391	-0.584	-0.586
52889.6166	-	-0.357	-0.713	-1.068	-1.365	-0.533	-0.522
52890.6166	0.027	-0.367	-0.753	-1.068	-1.361	-0.502	-0.552
52904.5900	0.038	-0.398	-0.769	-1.096	-1.433	-0.517	-0.597
52922.5165	0.043	-0.382	-0.736	-1.086	-1.379	-0.559	-0.604
52935.5517	0.049	-0.384	-0.744	-1.083	-1.382	-0.541	-0.594
52950.4901	-	-0.423	-0.763	-1.142	-1.385	-0.596	-0.577
52985.3382	0.032	-0.378	-0.771	-1.101	-1.409	-	-
53008.5002	-	-0.378	-0.714	-1.086	-1.351	-	-
53026.5686	-	-0.421	-0.764	-1.125	-	-	-
53056.3132	0.051	-0.352	-0.738	-1.090	-1.381	-	-
53069.4435	0.059	-0.397	-0.749	-1.114	-1.373	-	-
53077.4511	0.051	-0.417	-0.769	-1.121	-1.383	-	-
53094.3720	0.009	-0.349	-0.779	-1.103	-1.403	-	-
53110.3685	0.029	-0.367	-0.758	-1.093	-1.428	-	-
53122.3420	-	-0.409	-0.760	-1.087	-1.344	-	-
53273.6200	-	-0.390	-0.741	-1.098	-1.382	-	-
53291.5840	0.015	-0.386	-0.771	-1.118	-1.407	-	-

Table 10: $UBV(RI)_C$ data obtained with the SBIG STL 11000 CCD camera. The columns with HJD+ denote the fraction of the day.

HJD	$HJD+$	ΔU	$HJD+$	ΔB	$HJD+$	ΔV	$HJD+$	ΔR_C	$HJD+$	ΔI_C
2453449	.4107	-0.131	.4380	-0.373	—	—	—	—	—	—
2453463	.3898	-0.128	.3955	-0.378	.4031	-0.716	.4066	-0.993	.4107	-1.329
2453477	—	—	.3587	-0.389	.3556	-0.725	.3684	-1.019	.3709	-1.339

Table 11: $UBV(RI)_C$ data of the 2006 secondary eclipse obtained with the SBIG STL 1001 CCD camera. The columns with HJD+ denote the fraction of the day.

HJD	$HJD+$	ΔU	$HJD+$	ΔB	$HJD+$	ΔV	$HJD+$	ΔR_C	$HJD+$	ΔI_C
2453648	.6597	-0.110	.6614	-0.381	.6622	-0.748	.6638	-1.032	.6644	-1.375
2453745	.6161	-0.152	.6129	-0.388	.6104	-0.750	.6185	-1.036	.6196	-1.379
2453760	—	—	.4652	-0.388	.4591	-0.751	.4784	-1.028	.4805	-1.382
2453789	.2514	-0.116	.2476	-0.381	.2451	-0.750	.2551	-1.027	.2582	-1.389
2453799	.3832	-0.137	.3861	-0.385	.3873	-0.743	.3887	-1.024	.3894	-1.366
2453801	.3573	-0.135	.3602	-0.376	.3612	-0.744	.3621	-1.022	.3630	-1.374
2453816	.3272	-0.135	.3267	-0.389	.3348	-0.746	.3307	-1.016	—	—
2453818	.3875	-0.147	.3889	-0.390	.3893	-0.754	.3898	-1.005	.3901	-1.337
2453819	.3655	-0.127	.3683	-0.368	.3700	-0.725	.3713	-0.983	.3723	-1.321
2453828	—	—	.3327	-0.328	.3281	-0.643	.3465	-0.896	.3492	-1.203
2453829	.2706	-0.103	.2652	-0.323	.2613	-0.647	.2741	-0.889	.2908	-1.194
2453829	—	—	—	—	.2931	-0.642	.2898	-0.884	—	—
2453831	.3043	-0.102	.3072	-0.335	.3007	-0.659	.3081	-0.894	.3089	-1.208
2453832	—	—	.3913	-0.342	.3922	-0.664	.3928	-0.904	.3933	-1.231
2453833	—	—	.3907	-0.350	.3796	-0.688	.3808	-0.948	.3819	-1.250
2453837	—	—	—	—	.3607	-0.673	—	—	—	—
2453844	—	—	.3568	-0.394	.3523	-0.738	.3603	-1.032	.3617	-1.368
2454025	.4877	-0.135	.4827	-0.386	.4812	-0.741	.4913	-1.035	.4922	-1.368
2454066	.4471	-0.144	.4389	-0.373	.4354	-0.738	.4406	-1.029	.4418	-1.376
2454120	.6090	-0.169	.6044	-0.425	.6031	-0.794	.6066	-1.043	.6075	-1.376
2454128	.3383	-0.136	.3435	-0.421	.3310	-0.770	.3469	-1.030	.3496	-1.371
2454188	—	—	.2808	-0.431	.2827	-0.773	.2847	-1.047	.2882	-1.383
2454207	.3560	-0.157	.3519	-0.449	.3497	-0.795	.3483	-1.047	.3466	-1.382

Table 12: Radial velocity data obtained by R.F. Griffin
and A. Duquennoy.

Hel. Date	HJD–2400000	Velocity [$km s^{-1}$]		Source*	Weight
		prim.	sec.		
1988 Nov. 3.21	47468.71	−19.0	−	OHP	1
1988 Nov. 7.19	47472.69	−18.4	−	OHP	1
1988 Dec. 6.09	47501.59	−17.0	−	Cambridge-old	1/8
1988 Dec. 13.04	47508.54	−16.5	−	Cambridge-old	1/8
1988 Dec. 20.04	47515.54	−14.0	−	Cambridge-old	1/8
1989 Jan. 5.03	47531.53	−15.3	−	Cambridge-old	1/8
1989 Jan. 17.98	47544.48	−12.5	−	Cambridge-old	1/8
1989 Feb. 24.18	47581.68	−10.8	+6.1	ESO	1
1989 Mar. 26.84	47612.34	−8.9	+0.4	OHP	1
1989 Apr. 29.82	47646.32	−7.0	+0.6	OHP	1
1989 Oct. 30.16	47829.66	−0.7	−14.9	OHP	1
1989 Nov. 17.14	47847.64	+2.6	−	Cambridge-old	1/8
1989 Dec. 23.04	47883.54	+1.3	−	Cambridge-old	1/8
1990 Jan. 14.01	47905.51	+2.2	−	Cambridge-old	1/8
1990 Jan. 30.02	47921.52	+2.1	−18.4	OHP	1
1990 Feb. 12.14	47934.64	+1.5	−18.9	ESO	1
1990 Apr. 4.84	47986.34	+3.2	−	Cambridge-old	1/8
1990 Oct. 7.20	48171.70	+6.6	−	Cambridge-old	1/8
1990 Dec. 4.13	48229.63	+7.2	−	Cambridge-old	1/8
1991 Jan. 26.01	48282.51	+6.6	−22.6	OHP	1
1991 Mar. 13.85	48329.35	+6.5	−	Cambridge-old	1/8
1991 Apr. 3.87	48350.37	+3.7	−	Cambridge-old	1/8
1991 Oct. 29.16	48558.66	−30.4	+30.2	OHP	2
1991 Dec. 19.04	48609.54	−32.5	+33.5	OHP	2
1992 Jan. 14.01	48635.51	−29.9	+30.2	OHP	2
1992 Jan. 18.00	48639.50	−29.1	+30.3	OHP	2
1992 Jan. 24.06	48645.56	−28.4	+31.0	OHP	2
1992 Feb. 27.30	48679.80	−24.1	+22.3	DAO	2
1992 Apr. 22.85	48735.35	−18.5	+14.0	OHP	1
1992 Aug. 16.13	48850.63	−	−9.0	OHP	0
1992 Aug. 17.13	48851.63	−	−9.1	OHP	0
1992 Dec. 18.07	48974.57	−	−4.8	OHP	0
1993 Feb. 15.93	49034.43	−	−3.4	OHP	0
1993 Mar. 22.86	49069.36	−1.4	−16.8	OHP	1
1993 Apr. 20.83	49098.33	−0.4	−15.5	OHP	1
1993 Aug. 30.16	49229.66	−	+1.5	OHP	0

Hel. Date	HJD–2400000	Velocity [km s ⁻¹]		Source*	Weight
		prim.	sec.		
1993 Sep. 12.14	49242.64	+4.2	−10.6	OHP	1
1993 Nov. 6.34	49297.84		+3.3	OHP	0
1994 Jan. 3.05	49355.55	+6.4	−	OHP	1
1994 Feb. 19.88	49403.38	+6.1	−18.7	OHP	1
1994 Apr. 30.84	49473.34		+5.7	OHP	0
1994 Dec. 12.13	49698.63	−1.6	−17.0	OHP	1
1995 Jan. 5.06	49722.56		−4.4	OHP	0
1996 Jan. 1.08	50083.58		−10.1	OHP	0
1996 Mar. 31.87	50174.37		−6.4	OHP	0
1996 Dec. 16.07	50433.57		+1.5	OHP	0
1997 Jan. 26.03	50474.53	+2.8	−15.0	OHP	1
1997 Sep. 11.16	50702.66		+5.2	OHP	0
1997 Dec. 21.06	50803.56	+6.5	−15.9	OHP	1
2000 Jan. 9.02	51552.52	−1.5	−9.5	Cambridge	1
2000 Feb. 28.86	51603.36	−0.7	−15.9	Cambridge	1
2000 Apr. 6.85	51641.35	+1.3	−11.5	Cambridge	1
2000 Nov. 13.17	51861.67	+5.4	−15.4	Cambridge	1
2001 Jan. 7.02	51916.52	+5.6	−18.0	Cambridge	1
2001 Feb. 13.93	51954.43	+6.3	−20.0	Cambridge	1
2001 Nov. 14.20	52227.70	−2.7	−13.8	Cambridge	1
2001 Dec. 12.11	52255.61		−5.9	Cambridge	0
2001 Dec. 22.05	52265.55	−9.2	−1.7	Cambridge	1
2002 Jan. 17.99	52292.49	−17.7	+18.2	Cambridge	1
2002 Jan. 24.97	52299.47	−20.2	+17.2	Cambridge	1
2002 Feb. 5.98	52311.48	−23.8	+26.0	Cambridge	2
2002 Feb. 16.90	52322.40	−27.5	+25.7	Cambridge	2
2002 Mar. 1.88	52335.38	−29.5	+31.2	Cambridge	2
2002 Mar. 9.90	52343.40	−31.3	+29.6	Cambridge	2
2002 Mar. 27.87	52361.37	−33.1	+34.7	Cambridge	2
2002 Apr. 6.86	52371.36	−33.0	+34.4	Cambridge	2
2002 Apr. 23.85	52388.35	−32.2	+35.2	Cambridge	2
2002 Oct. 24.18	52571.68	−13.2	−	Cambridge	1
2002 Nov. 7.20	52585.70	−12.3	−	Cambridge	1
2003 Jan. 6.01	52645.51	−8.3	−4.1	Cambridge	1
2003 Dec. 15.13	52988.63	+2.8	−14.6	Cambridge	1
2004 Feb. 27.94	53063.44	+4.0	−18.2	Cambridge	1
2005 Jan. 11.03	53381.53	+5.6	−18.6	Cambridge	1
2005 Nov. 25.16	53699.66	−26.4	+27.9	Cambridge	2
2005 Dec. 28.09	53732.59	−22.4	+23.5	Cambridge	2

Hel.	Date	HJD–2400000	Velocity [km s ⁻¹]	Source*	Weight
			prim. sec.		
2006	Feb. 20.93	53787.43	–17.0 +9.3	Cambridge	1
2007	Apr. 10.87	54201.37	+1.5 –12.2	Cambridge	1

Description for the table 12:

*Sources:

HPO - Coravel at Haute-Provence Observatory,

Cambridge-old - the old original radial-velocity spectrometer at Cambridge, with which Griffin first developed the cross-correlation method of measuring velocities (ApJ 148, 465, 1967),

Cambridge - Coravel instrument currently working at Cambridge Observatory,

DAO - instrument at Dominion Astrophysical Observatory,

ESO - another spectrometer similar Coravel.

The velocities written between the columns for the primary and secondary have been reduced as if the system were single-lined and the zero weight were applied in those cases.

The data before 1992 Aug. 16 were published already by Griffin & Duquennoy in 1993, but now they have been corrected by Dr Griffin and are presented here once again.

Table 13: Radial velocity data obtained from Rozhen Observatory spectra.

Date	JD–2400000	Velocity [km s ⁻¹]	Weight
		prim. sec.	
2005 Jan. 20	53391.31	+5.5 ± 0.8 –18.2 ± 1.3	1
2006 Apr. 14	52581.70	–12.5* ± 0.9	1

* this is measurement of the blend of primary and secondary but the weight one was applied for calculations